(4)

MRL-R-1146

AR-005-671

DEPARTMENT OF DEFENCE

DEFENCE SCIENCE AND TECHNOLOGY ORGANISATION

MATERIALS RESEARCH LABORATORY

MELBOURNE, VICTORIA

REPORT

MRL-R-1146

CORROSION OF HIGH-DENSITY SINTERED TUNGSTEN ALLOYS
PART 3: ELECTROCHEMICAL TESTS

J.J. Batten, S.A. Bombaci, W.N.C. Garrard,
B.T. Moore and B.S. Smith

Approved for Public Release

DSTO MRL
MELBOURNE

DECEMBER 1988

DEPARTMENT OF DEFENCE

MATERIALS RESEARCH LABORATORY

REPORT

MRL-R-1146

CORROSION OF HIGH-DENSITY SINTERED TUNGSTEN ALLOYS
PART 3: ELECTROCHEMICAL TESTS

J.J. Batten, S.A. Bombaci, W.N.C. Garrard,
B.T. Moore and B.S. Smith

ABSTRACT

The corrosion behaviour of tungsten and high-density tungsten alloys (W ≥ 90 weight %) has been examined electrochemically through anodic polarization measurements, instantaneous corrosion rate measurements, galvanic coupling, and surface potential mapping. In the anodic polarization tests, pure tungsten and the four alloys studied underwent transitions from an active state to a state where any further increase in potential produced no further increase in current. The presence of chloride ions increased corrosion rates.

Predictions of likely trends in corrosion rates from the above electrochemical tests were not in complete agreement with those obtained by the long-term immersion tests. Similarly, a consistent prediction of the likely nature of the corrosion products that would result from long-term immersion testing was not obtained from the above studies. Predictions about which alloys would be susceptible to a crevice effect were in agreement with the immersion testing results, namely those alloys not containing Cu would be the most susceptible.

Some insight into the nature of the corrosion mechanism is afforded by the work on galvanic coupling and surface potential mapping: this supported the view that galvanic corrosion plays a part in the corrosion process.

POSTAL ADDRESS: *Director, Materials Research Laboratory*
P.O. Box 50, Ascot Vale, Victoria 3032, Australia

CONTENTS

CONTENTS
(continued)

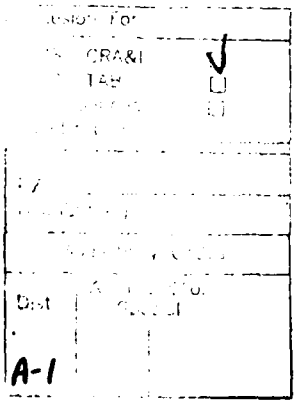

CORROSION OF HIGH-DENSITY SINTERED TUNGSTEN ALLOYS

PART 3: ELECTROCHEMICAL TESTS

1. INTRODUCTION

The previous work [1-4] was concerned with a study of the corrosion of tungsten and four high-density sintered tungsten alloys by long-term immersion in distilled water and in sodium chloride solution. The main points arising from that work were:

(a) Corrosion rates of alloys not containing copper were always less than those containing copper.

(b) Corrosion rates were less in sodium chloride solution than in distilled water.

(c) Corrosion products arising from corrosion in distilled water consisted predominantly of tungsten, while those in sodium chloride solution mainly contained binder elements.

(d) There was a crevice effect in sodium chloride solution with those alloys not containing copper.

The work reported here was aimed at more fully evaluating the corrosion behaviour of the various tungsten alloys. Corrosion characteristics were determined by potentiostatic polarization methods, by instantaneous corrosion rate measurements, by galvanic coupling experiments and by surface potential mapping.

In other electrochemical studies of tungsten and high-density tungsten alloys [5, 6, 7], anodic polarization curves have been obtained in (aerated) sodium chloride solution. In general, these results showed that pure tungsten and all the alloys studied underwent active-passive transitions. Corrosion rates for the tungsten alloys in aqueous solutions, obtained by Tafel slope extrapolation, were generally increased by the presence of chloride ions whereas that of pure tungsten was unaffected. Further, in

sodium chloride solution from pH 4 to 9, alloys containing similar percentages of Ni and Fe (some not containing copper) all had similar corrosion rates. In the absence of chloride ions, however, those alloys containing copper had much higher corrosion rates. Corrosion products were not analyzed.

In the one relevant study involving galvanic coupling [8], pure tungsten was coupled with a "binder phase" that did not contain tungsten. However, in an alloy, the binder phase may contain up to 30% tungsten [1-4]. Thus, the relevance of such results to the actual corrosion mechanism of an alloy is questionable.

In the above electrochemical tests, little attempt was made to correlate the results with those obtained from long-term immersion experiments. It is clear that there is a dichotomy between our immersion results [1-4] and the above electrochemical results, even when the slight difference in the chemical composition of the alloys used in the two sets of tests is taken into consideration.

The present paper reports on the corrosion behaviour (as examined by standard electrochemical techniques) of tungsten and the same sintered tungsten alloys as those used in the immersion experiments [1-4]. The tests were conducted in distilled water and sodium chloride solution. Both aerated and de-aerated solutions were used, and the work is correlated with the results of long-term immersion tests [1-4].

2. EXPERIMENTAL

2.1 Anodic Polarization Studies*

Specimens for this study were polished with 600A aluminium oxide paper, rinsed with distilled water, toluene vapour degreased and air dried. The exposed area of each electrode was 1 cm^2 and the excess surface area was masked with an alkyd varnish [10].

The solutions used were unbuffered distilled water and 3.5% sodium chloride solution. These were de-aerated and aerated by bubbling nitrogen and oxygen, respectively, through them. The initial pH of the solutions was in the range 5.5 to 5.7.

Polarization measurements were made using the potential sweep method of potentiostatic polarization [11]. The electrode potential was continuously changed at a constant rate 0.2 mV s^{-1} using a PAR 174A polargraphic analyser to anodically polarize the electrode and at the same time record the current. Polarization curves were recorded on an MFE 815M X-Y recorder and a HP 3478A multimeter was used to monitor potentials. Potentials were measured against a saturated calomel reference electrode (SCE). Platinum was used as an auxillary electrode. The specimens were allowed to

* For definition of terms used see Reference 9.

remain in the solution for 1 h to achieve a steady-state corrosion potential before applying and sweeping the potential from -650 to +2000 mV versus SCE.

2.2 Instantaneous Corrosion Rate Studies

To determine corrosion rates by extrapolation of Tafel slopes to the corrosion potential, use was made of the instantaneous corrosion rate measurement technique [12]. In this, the instantaneous corrosion rate of the alloy was measured by a computerised polarization pulse method in cells with aerated 3.5% sodium chloride solution as the corroding electrolyte. Voltage pulses (alternately anodic and cathodic up to ± 30 mV) are applied to the electrodes and consequent changes in cell current measured. Mathematical regression analysis was then used to produce values for corrosion resistance, Tafel slope parameters (both anodic and cathodic) and finally, corrosion current and hence metal loss rate due to corrosion was calculated.

2.3 Electrochemical Cell Studies

Three galvanic couples were investigated, namely tungsten to AUS binder, tungsten to AUS alloy, and AUS alloy to AUS binder, using the technique outlined in ASTM G71 [13]. The specimens were polished to 400 grit silicon carbide and the unexposed surface was masked with an epoxy resin. Electrical connection was made to the specimens using a cured silver-loaded epoxy. The electrodes were degreased and immersed either in 5% sodium chloride solution, or in distilled water, using individual glass cells containing three litres of solution for each couple. The cells were at ambient temperature (about 20°C).

Corrosion was monitored using a zero resistance ammeter, with potential measurements referenced to saturated calomel electrodes immersed in each cell. The data was logged using a two-pen recorder. The exposed areas of the tungsten and AUS-alloy electrodes were 4 and 1 cm^2, respectively, while that of the binder phase was either 1 or 0.3 cm^2. Prior to forming the galvanic couple, the specimens were allowed to remain in the solution for as much as 72 hours to let the potential reach a steady-state corrosion potential.

2.4 Surface Potential Mapping Studies

In the isopotential contouring system used for monitoring surface corrosion [14], a small reference electrode (40 μm diameter) is passed across the corroding specimen close to its surface (solution gap of 37 μm), and the potential difference relative to another fixed reference electrode is recorded. The changes in potential are associated with the current flow between anodic and cathodic sites. Thus the potential profile reflects the ion current density in the vicinity of the corroding surface.

The scanning was accomplished by moving the probe in a two-dimensional raster pattern across the mounted specimen. All aspects of the experiment, including probe movement, data acquisition, data processing and presentation of the data, were

under computer control. Both the fixed and scanning reference electrodes were Ag/AgCl electrodes.

3. RESULTS

3.1 Anodic Polarization Studies

3.1.1 Pure tungsten

Figure 1 shows the anodic behaviour of pure tungsten in unbuffered distilled water and in unbuffered 3.5% sodium chloride solution, both solutions being either aerated or de-aerated. Corrosion potentials [9, 11] are listed in Table 1, where these potentials were measured soon after immersion (see later). Generally, it will be seen that these corrosion potentials become more active (i.e. more negative [9]) in the de-aerated solutions, and are more active in both the sodium chloride solutions.

It can be seen from Figure 1 that the dissolution of tungsten in all solutions, except aerated water, has an initial passive region. After this, with all solutions, there is an active region [11] and then the tungsten undergoes transitions to a region where further increase in potential produces no further increase in current (hereafter referred to as the limiting current (LC) region). The maximum dissolution current density (i.e. the current density (or corrosion rate) at the onset of the LC region) for the sodium chloride solutions is higher than those for distilled water (Table 1). But, as figure 1 shows, there is a distinct "knee" in the sodium chloride curve, so that the limiting current densities are much the same in all solutions. Further, the potential at which the LC region begins shows little variation (Table 1).

The above LC region is not a true passivation region however, for although the corrosion rate increases only marginally with potential, corrosion continues at a fairly rapid rate. None of these polarization curves shows a transpassive region [9, 11], i.e. a region after the above pseudo-passivation region where an increase in potential produces an increase in current.

3.1.2 Alloy AUS (95%W, 3.5%Ni, 1.5%Fe)

The effect on the anodic polarization behaviour of alloying tungsten with nickel and iron is illustrated in Figure 2, and the corresponding corrosion potentials are listed in Table 1. Again, the order of activity of these potentials is:- de-aerated sodium chloride > de-aerated distilled water > aerated sodium chloride > aerated distilled water. This alloy undergoes transitions from the active state to the LC region (as defined above) in both distilled water and in sodium chloride solution, although in this latter case the LC region is somewhat questionable.

In distilled water, the regions of active dissolution and limiting current are virtually identical with those of pure tungsten and are, therefore, attributed to the

tungsten in the alloy. On the other hand, in sodium chloride solution both the active and LC regions of AUS are somewhat different from those that occurred for pure tungsten in this solution. Further, unlike tungsten, there is a transpassive region (as defined above). These differences are attributed to the alloying elements in the alloy, while the LC region could be attributed to tungsten.

Thus the nature of these curves in distilled water suggest that the corrosion process is much the same as that which occurs on pure tungsten, while those in sodium chloride solution suggest that the corrosion process is more complex.

SEM examination of the corroded surfaces indicated that the main attack in sodium chloride solution had occurred on the binder phase, both on the exposed surface and also under the alkyd varnish (see Experimental). Similar attack also took place in distilled water, but there was also some attack on the tungsten particles.

3.1.3 Alloy UK(Fe) (90%W, 5%Ni, 5%Fe)

The influence on the anodic polarization curve of increasing the iron to nickel ratio in these alloys is shown in Figure 3. The respective corrosion potentials are listed in Table 1, where it will be seen that their order of activity is the same as that found for W and AUS.

In distilled water, the anodic behaviour is much the same as that for W and AUS, in particular the current densities and potentials at the onset of the LC region and the shape of the curves in the active region. As with AUS, there appears to be a tendency for the development of a transpassive region.

In sodium chloride solution, however, the behaviour is very different from that of either W or AUS. In this case there is only a very small LC region at high current density in de-aerated sodium chloride, but in general the alloy undergoes active dissolution at all potentials to quite high current densities.

SEM examination of the corroded surfaces indicated that attack was predominantly on the binder phase of the exposed surface in all solutions, but the extent of attack in distilled water was only slight.

3.1.4 Alloy UK(Cu) (90%W, 7.5%Ni, 2.5%Cu)

The effect on the anodic polarization curve of replacing the iron in these alloys with copper is illustrated in Figure 4. The respective corrosion potentials, listed in Table 1, are in the order noted for the other alloys. In all solutions, however, there have been radical changes in the form of the anodic polarization curves. The main features of these curves are listed below:

(a) In aerated distilled water, after the active region there is an ill-defined LC region - in fact corrosion current continues to increase regardless of the applied potential.

(b) In de-aerated distilled water there appears to be a transition from the active state to the LC region, but the current density at the onset of this LC region is rather high.

(c) In the sodium chloride solutions, the transition to the LC region occurs at a very high current density, and the LC region only extends over a small potential range.

SEM examination of the corroded surfaces indicated that in sodium chloride solution corrosion had mainly occurred in the binder phase on both the exposed surface and under the alkyd varnish. A similar pattern of corrosion occurred in distilled water, but the extent of attack was not as great.

3.1.5 Alloy US (97%W, 1.6%Ni, 0.7%Fe, 0.5%Cu, 0.1%Co)

This alloy contains nickel, iron and copper (and cobalt as a minor constituent), and the effect of these elements on the anodic polarization curve is presented in Figure 5. The respective corrosion potentials are listed in Table 1, and their order of activity is the same as found previously.

This alloy undergoes a transition to the LC region in all solutions. In the absence of chloride ions the anodic polarization curves are very similar in shape to those of pure tungsten (e.g. the active region, the current density at the onset of the LC region). Unlike tungsten, however, cessation of the LC region does appear to occur, so forming a transpassive region. Nevertheless it is concluded that its behaviour in distilled water is largely due to tungsten, as might be expected from its composition (i.e. 97%W).

In the presence of chloride ions, however, the behaviour more closely approximates that of UK(Cu). Both alloys have transitions from the active state to the LC region that commence at about the same potential and current density. This similarity is attributed to the presence of copper. The very large current density required for this alloy to have a LC region (see Table 1) suggests that it would have little resistance to corrosion in this medium.

SEM examination of the corroded specimens indicated that in all solutions, the attack had mainly taken place on the binder phase.

3.1.6 AUS BINDER (23%W, 55%Ni, 21%Fe)

Figure 6 shows the anodic behaviour of the binder phase in the alloy AUS and the effect on it of chloride ions. An initial passive region is observed in all curves except that for aerated sodium chloride. The corrosion potentials for this binder phase alloy are listed in Table 1, and again the order of activity is the same as for all the alloys tested.

In distilled water, this material undergoes ill-defined transitions to the LC region and it appears that their onset is influenced by the aeration of the solution. In sodium chloride solution, however, there are well-defined LC regions and these extend over a small potential range and are at fairly high current density values: this behaviour is somewhat analogous to that of pure nickel in sodium chloride solution at a pH of 4 [5].

3.2 Instantaneous Corrosion Rate Studies

Corrosion rates were obtained, using the computerized electrochemical technique [12], for pure tungsten, the four alloys AUS, UK(Fe), UK(Cu), US, and the AUS binder material. The results are presented in Table 2, together with results obtained previously by immersion testing for seventy days [1-4]. Both the above techniques yield the same general result, namely that the corrosion rate for all the metal samples is low, generally being less than 0.5 mil/yr (i.e. less than 12.5 μm/yr). Individual agreement between the results of the two test methods can only be regarded as "fair", however, although there does appear to be a trend. Thus, for example, for those alloys not containing copper the instantaneous rate > immersion rate, while the reverse is the case for those alloys containing copper. In [1-4] it was also noted that often the behaviour of these materials to a particular stimulus (e.g. crevice) could be grouped in a like manner.

3.3 Electrochemical Cell Studies

3.3.1 Variation of corrosion potential with time of immersion

The corrosion potentials of uncoupled electrodes of pure tungsten, the Australian-alloy binder phase, and the Australian alloy (AUS) in 5% sodium chloride solution and in distilled water are listed in Table 3. This shows large fluctuations in the corrosion potentials with time of immersion (particularly in distilled water). However, a single value may be selected to represent the typical steady-state corrosion potential (mV) (SCE) for each metal system as follows:

	W	Binder	AUS
Sodium Chloride Solution	-250	-440	-340
Distilled Water	-250	-320	-350

As the Australian alloy AUS is composed of tungsten particles in a binder phase, it could be expected that its corrosion potential would lie between those of its composite phases. This is the case in sodium chloride solution, i.e. AUS is always more negative than pure tungsten but less negative than the binder. In distilled water, however, although it is more negative than tungsten, often it is also more negative than the binder.

To gain a better appreciation of the behaviour of corrosion potentials in distilled water, the above work was repeated with the time of immersion extended and the experiment more closely monitored. These results are given in Figure 7 where it will be seen that after a settling down period of about seven days (during which several

reversals in the relative order of the corrosion potentials occurred), the corrosion potential for AUS was always between that of pure tungsten and the binder. After about one hundred days, a pseudo-steady state is reached and the corrosion potentials of AUS and binder are almost identical, but all three systems have become much more negative.

During the course of the above study, the pH of the solutions rose. The initial pH was about 5.5 whereas at forty days it was 6.5 (for tungsten) and about 7 (for AUS and the binder). At 160 days these figures were about 7 and 7.5 respectively.

3.3.2 Galvanic corrosion studies in 5% sodium chloride solution

The data for these experiments are presented for each galvanic couple in Table 4 together with the relative surface areas of the electrodes.

3.3.2.1 Electrochemical cell: Tungsten/Binder phase

(a) Relative surface area of electrodes 4:1

With both the static and stirred systems, the mixed potential remained stable throughout the experiment and was between that of the corrosion potentials of the two uncoupled (and unstirred) electrodes (Table 4). Thus it is assumed that the polarity would not have changed during the experiment and that the binder phase remained the anode (i.e. the metal with the more active corrosion potential).

The behaviour of the galvanic current indicates that the stirred system stabilized more quickly than the static system. Further, the stable galvanic current is somewhat influenced by agitation. It is possible, therefore, that the reaction is partially diffusion controlled.

(b) Relative surface area of electrodes 4:0.3

The response to the reduction in the surface area of the anode, i.e. binder phase, to one-third of that used previously was a corresponding reduction in the galvanic current of the electrochemical cell (Table 4). This does not necessarily mean, however, that the corrosion rate of binder phase going into solution has remained constant. Since galvanic current is a composite measurement it is difficult to deduce the individual electrode reaction rates unless one or more reactions can be eliminated. It will also be noted from Table 4 that the above reduction in the surface area of the anode resulted in the mixed potential approximating that of the uncoupled corrosion potential of the binder phase.

3.3.2.2 Electrochemical cell: Tungsten/AUS alloy (1:1)

It would be expected that in this cell the AUS alloy would be anodic to the tungsten because of the presence of the binder phase in the alloy. It will be seen from Table 4 that the mixed potential is between the corrosion potentials of the two uncoupled electrodes but is closer to that of the electrode AUS alloy. Again the stirred system stabilized more quickly than the static system, and stirring increased the galvanic current.

3.3.2.3 Electrochemical cell: AUS alloy/Binder phase (1:1)

In this cell it would be expected that the tungsten particles in the AUS alloy would make it cathodic to the binder. In this case the static mixed potential is identical with that of the corrosion potential of the uncoupled binder phase (Table 4). Unlike the above examples, the galvanic current is reduced quite markedly by stirring the sodium chloride solution. A possible explanation for this behaviour is that accumulated corrosion products on the surface catalyse the corrosion process (cf. [15]).

3.3.3 Galvanic corrosion studies in distilled water

The data for these experiments are presented for each galvanic couple in Table 5 together with the relative surface areas of the electrodes.

3.3.3.1 Electrochemical cell: Tungsten/Binder phase

(a) Relative surface area of electrodes 4:1

In the static system the mixed potential is between the corrosion potentials of the two uncoupled electrodes and is close to that for tungsten (see Table 5). Thus, the binder phase remained the anode throughout the course of the experiment. Further, in this case, the stable galvanic current of the cell is not significantly affected by stirring. This lack of a strong effect may be due to electrolyte resistance (i.e. distilled water). Similarly, stirring has had a marked affect on the stable mixed potential and it now lies outside the range of the corrosion potentials of the two uncoupled (and unstirred) electrodes and is more noble than tungsten (Table 5) but lies within the range of tungsten potentials shown in Figure 7.

(b) Relative surface area of electrodes 4:0.3

There have been two main responses to this change in the surface area ratio (see Table 5). First, the mixed potential is not now significantly influenced by the solution being stirred. Secondly, there has been a dramatic increase in the stable galvanic current (e.g. 0.5 to 11 μA).

3.3.3.2 Electrochemical cell: Tungsten/AUS alloy (1:1)

In this case (Table 5) the mixed potential lies between the corrosion potentials of the two uncoupled electrodes in both the static and stirred systems. Thus the AUS alloy remained the anode throughout the reaction. Stirring, however, does make the mixed potential become more noble. Table 5 also indicates that the stable galvanic current is unaffected by the agitation.

3.3.3.3 Electrochemical cell: AUS alloy/Binder phase (1:1)

Here (see Table 5) the mixed potential is either equal to, or more noble than, the uncoupled (and unstirred) corrosion potential of the more noble electrode (namely AUS alloy). Also in this case the galvanic current is very low.

3.4 Surface Potential Mapping Studies

The scanning reference electrode technique is used for mapping the distribution and severity of localized corrosion, and to monitor the development of corrosion sites and changes in the corrosion rate under a wide range of conditions. In the previous section it was demonstrated that an electrochemical cell was created when samples of tungsten and the binder phase were immersed in the same solution and connected electrically. Therefore, such galvanic corrosion should be amenable to study by this surface potential mapping technique. The potential contour maps give close to a real time measure of corrosion.

3.4.1 On samples consisting of AUS binder and pure tungsten

3.4.1.1 Sample: tungsten button with a centrally located insert of AUS binder

The isopotential contour map obtained when the reference electrode traversed a pure tungsten button (about 9 mm diameter) with a centrally located, firmly fitted, insert of AUS binder (about 2.5 mm diameter) is shown in Figure 8(a) where the time of immersion in the 2.5×10^{-4} M sodium chloride solution was about 1 hour. This sample was initially polished on 1200 grade aluminium oxide paper. The figure shows a circular region (it appears oval because of the method of plotting) with a steep potential gradient corresponding to the interface between the binder and the tungsten. The step between each of the above contours is about 4 mV. This contour map is interpreted to indicate that most of the corrosion is taking place on the binder in an area close to the tungsten/binder interface.

There is a central area of fairly uniform electric field in the middle of the binder. Although the potential in this region is not as large as the maximum potential in the peripheral area it is still high, indicating that here also some corrosion is taking place. The moderately low uniform potential over the tungsten surface indicates that here little, or no, corrosion is taking place.

The development of the corrosion pattern, four hours after immersion, is evident in Figure 8(b). The main difference between these two figures is the development of more distinct localized corrosion sites located in the area just inside the region of steep potential gradient.

Comparison of the above isopotential contour map with the location of corrosion products visible on the micrograph of the surface (Figure 9) shows that the potential scanning technique gives results which accurately reflect the surface corrosion of the specimen. It is clear that the concentric ring area corresponds to anodic corrosion centres on the binder.

Analysis of the corrosion products (about 40%W, 35%Ni, 25%Fe) deposited on the sample indicates that they consist predominantly of binder material, thus supporting the conclusions drawn from the above contour maps. It is pertinent that in a separate experiment with the binder material alone exposed to the above solution for the same time (4 hours), only very mild localized corrosion was noticeable on its surface.

Figures 9 and 10(a) show, however, that a crevice existed around part of the periphery of the binder insert, while in Figure 10(b) no such crevice is evident. Although this latter figure indicates that galvanic corrosion does occur when tungsten and AUS binder are connected in solution, Figure 10(a) could indicate that this system is also susceptible to attack by crevice corrosion.

After remounting the specimen such that the crevices between the tungsten and binder were filled with epoxy resin, the resulting contour map was similar to that obtained previously. Thus it is assumed that this system is not susceptible to attack by crevice corrosion and that the concentric ring pattern (Figure 8) is a result of bimetallic corrosion between these two metals.

3.4.1.2 Sample: "crevice free" AUS binder/tungsten couple

The aim of this investigation was to develop a tungsten/AUS binder galvanic couple system where the anodic and cathodic reaction sites were clearly separated and where crevices could not be formed between these two metals, and then to conduct scanning reference electrode studies on this galvanic couple. To achieve this a sample was prepared where tungsten and the AUS binder were mounted side-by-side and close together (but not touching) in bakelite moulding powder. An electrical contact was made between the back surfaces of these two metals using silver-loaded epoxy adhesive (see Figure 12).

The isopotential contour map obtained when the reference electrode traversed these two surfaces (separated by a wedge of mounting resin) is shown in Figure 11. This shows several concentric ring areas corresponding to active corrosion centres on the surface of the binder, while only little activity is apparent on the tungsten. Unlike the previous case, however, this time the active corrosion sites are not concentrated near the periphery of the binder but are spread at random over its surface. It is clear, however, that corrosion due to the galvanic couple is occurring, and that the binder surface is anodic to the tungsten surface.

The state of the surfaces of the binder and tungsten at the completion of the experiment (i.e. after 4 hours in the 2.5×10^{-4} M sodium chloride solution) is shown in Figures 12 and 13. Here localized corrosion sites are apparent on the binder while none is present on the tungsten surface. Figure 13 shows magnified micrographs of two of these sites. Figure 13(b) shows that despite the presence of a crevice between the moulding powder and the binder, crevice corrosion appears not to have taken place.

The chemical composition of the corrosion products on the surface (about 57%W, 15%Ni, 28%Fe) again indicates that it is mainly the binder that is corroding. Thus the binder surface is anodic to the tungsten surface, and again the surface potential mapping technique has reflected the corrosion pattern that is visible on the surfaces.

It is concluded that the observed corrosion is due to a bimetallic effect between the tungsten and the binder.

3.4.2 On the tungsten alloys AUS and US

Here the aim was to use actual high-density tungsten alloys and determine whether it was possible, using this surface potential mapping technique, to detect localized corrosion of binder between tungsten particles and/or localized corrosion of individual tungsten particles. To this end, cognizance needs to be taken of both the sensitivity (the ability to unambiguously determine very small corrosion currents originating from localized regions) and the resolution (the ability to distinguish between two anodic sites close to each other) of this technique. The resolution of this technique is usually considered to be about 50 μm (i.e. about the average size of tungsten particles in these alloys). Thus it was realized that there was only a slight chance of detecting these discrete, localized anodic and cathodic sites on the surface of these alloys.

3.4.2.1 Sample: the tungsten alloy AUS

The isopotential contour map across a small section of the surface of AUS is shown in Figure 14. Over this scanned area (which, in fact, is typical of that of the whole surface) there are only two anodic areas and the remainder of the area is a large cathodic site. After about the first day this pattern remained fairly constant throughout the 4-week test period. However, the contour map is not what we had hoped for, i.e. it does not show small discrete cathodic areas about the size of tungsten particles surrounded by a maze of anodic ribbon areas representing the corrosion of the binder.

The pattern of the contour map obtained above is reflected in the micrograph of the surface of the tungsten alloy AUS after immersion in distilled water for seventy days and after removal of corrosion products (Figure 15). There are large corroded areas (absence of polishing marks) surrounded by areas where little or no corrosion has taken place (polishing marks still evident). A similar pattern was obtained when AUS was exposed to 5% sodium chloride solution for seventy days.

3.4.2.2 Sample: the tungsten alloy US

The contour scan work was repeated using the alloy US for two reasons: first, when compared with AUS its corrosion rate is much faster and secondly, its tungsten particle size is bigger [1-4]. The contour map of this sample indicated that the surface was undergoing almost uniform corrosion, which is in accordance with visual and microscopic examination of the surface of the sample.

4. DISCUSSION

4.1 Anodic Polarization Studies

4.1.1 Shape of the anodic polarization curves

The anodic polarization curves show that pure tungsten and all the alloys studied undergo a transition from an active state to a LC region, albeit sometimes ill-defined, in the four solutions studied (distilled water and sodium chloride solution, aerated and de-aerated). The presence of chloride ions increases, often considerably, the current density at the onset of the LC region. This may be associated with the higher electrolyte conductivity due to the presence of chloride ions. Further, sometimes only a rather small LC region occurs in the presence of chloride ions.

In aerated distilled water (Figure 16), tungsten and the alloys AUS and US all showed the above transitions with similarly shaped curves. In the case of UK(Fe) and UK(Cu) the above trend is not quite so defined. In general, however, the behaviour of all the alloys in aerated distilled water can be attributed, to varying degrees, to the tungsten in the alloys.

The above behaviour is also evident in de-aerated distilled water (Figure 17). Here, with the exception of UK(Cu), all the alloys behaved in a like manner to that of tungsten. UK(Cu) has the highest (by many orders of magnitude) current density for the onset of the LC region and thus would be expected to have the poorest corrosion resistance in this environment.

This is not the case in either aerated or de-aerated sodium chloride solutions (Figures 18 and 19). The results clearly demonstrate that chloride ions in the solution can have a marked influence on the shape of the anodic polarization curves, presumably by having an influence on the mechanism of the reaction. This conclusion is substantiated by the results of the immersion tests [1-4].

The curves obtained in both the aerated and de-aerated sodium chloride solutions show similar characteristics for those alloys containing copper, while those for the Cu-free materials are somewhat different. Only the curves of AUS approach those for tungsten.

4.1.2 Corrosion rate predictions

Relative corrosion rate data may be obtained from these curves in two ways:

(a) From the corrosion current - the higher this current, the higher the corrosion rate.

(b) The magnitude of the current density at the onset of the LC region gives an indication of the corrosion resistance of the alloy [5] - the lower this figure the more corrosion resistant the material.

Relative corrosion rates in aerated solutions, estimated by the above means, did not rank the alloys in an order consistent with the results of immersion tests [1-4]. Similarly, use of the above two premises leads to the conclusion that the corrosion rates of these materials in aerated distilled water will be less than those in aerated sodium chloride solution - again a prediction not in agreement with the results from immersion tests [1-4].

4.1.3 Prediction of the nature of the corrosion products

The anodic polarization curves for all the alloys in aerated distilled water approximated that of tungsten. On this basis, it might be expected that the main corrosion product for all the alloys in aerated distilled water would be derived from tungsten. In aerated sodium chloride solution, only the curve for AUS approximated (and only roughly) that of tungsten, thus the main corrosion products might be expected to be typical of those that would arise from the binder. These predictions are in agreement with the results from the immersion tests [1-4].

4.1.4 Prediction of crevice corrosion susceptibility of these alloys

Premise: A crevice-effect will exist if the following two conditions are met.

First condition:

For a particular alloy there needs to be a large driving force between the two corrosion potentials 'aerated' and 'de-aerated'. This means that the corrosion potential of the alloy in de-aerated sodium chloride would need to be considerably more active than that in the aerated solution.

From Table 1 it will be seen that for all the alloys the corrosion potentials in de-aerated sodium chloride solution are more active than those in the aerated solution. In order of increasing magnitude, for the difference in potential mentioned above, the alloys would be listed in the following order:

$$UK(Cu) < W < US = AUS < UK(Fe)$$

In [1-4], a crevice effect was found for UK(Fe) and AUS, thus there appears to be some basis for the above condition.

Second condition:

For there to be a crevice effect for a particular alloy there needs to be a difference in the resistance to corrosion (where this is based on the passivation corrosion current) between aerated and de-aerated sodium chloride solutions. Using this condition gives the following sequence for increasing susceptibility to a crevice effect:

$$(W = UK(Cu) = US \text{ (all little tendency)}) < AUS < UK(Fe)$$

The premise therefore leads to the conclusion that if there is a tendency for a crevice effect, then it might be exhibited by the alloys UK(Fe) and AUS. This was found experimentally [1-4].

4.2 Instantaneous Corrosion Rate Studies

These measurements (see Table 2) group the copper-containing alloys (UK(Cu), US) as more corrosion resistant than those not containing copper. This trend is contrary to that found by long-term immersion testing [1-4]. However, the magnitudes of the corrosion rates obtained by the two methods are comparable, i.e. they would all be classed as 'very low'. These instantaneous corrosion rate measurements gave a wide scatter in the results which could indicate that the electrodes take a long time to come to equilibrium after the voltage-pulse disturbance. Thus the technique of measurement could upset the electrode equilibrium, even though the voltage perturbations are small. This difficulty probably only reflects the complexity of the corrosion process on these alloys.

4.3 Electrochemical Cell Studies

The results can be examined on the premise that the tungsten alloy AUS is composed of many thousands of little galvanic couples, where one electrode of each couple consists of the binder phase and the other consists of tungsten particles.

4.3.1 Significance of the corrosion potential studies

The results have shown (Table 3 and Figure 7) that the corrosion potential of the binder is always more active than that of tungsten, particularly so in sodium chloride solution. Hence, if these two corroding metals are galvanically coupled, the corrosion rate of the binder should be accelerated and that of the tungsten should be retarded. Thus it could be anticipated that the predominant source of corrosion products should result from corrosion of the binder and this is the case for experiments in sodium chloride solution [1-4].

4.3.2 Significance of the corrosion rate studies

On the basis that the galvanic current gives some measure of the extent of reaction taking place on the anode (the binder phase), then for the galvanic cell comprising tungsten/binder phase, the relationship of binder corrosion products to tungsten particle corrosion products might be anticipated to be higher in sodium chloride solution (where the galvanic current is higher) than in distilled water. Extrapolating this concept to the dissolution of the alloy AUS would yield the conclusion that the corrosion products should consist of a higher proportion of binder phase products in sodium chloride solution than found in distilled water - in agreement with the experimental result.

4.4 Surface Potential Mapping Studies

The aims of this work were, first to confirm the existence of bimetallic corrosion occurring with the electrochemical cell W/AUS binder, secondly to demonstrate that in this cell the binder was anodic to the tungsten, and thirdly to ascertain whether the contour mapping technique had sufficient resolution to detect localized corrosion occurring on the binder phase in actual high-density sintered tungsten alloys. The first two aims were successfully achieved. However, using this technique, it was not possible to detect any localized corrosion.

4.5 Corrosion Mechanism

In earlier studies [3, 4] it was suggested that corrosion in these alloys results from a bimetallic reaction, with the tungsten grains and the binder phase acting as electrodes. For the AUS alloy it was predicted that the binder phase would be anodic with respect to the tungsten grains. These predictions have been substantiated by the present work.

5. CONCLUSIONS

The behaviour of tungsten and four high-density sintered tungsten alloys has been studied by various electrochemical techniques. As indicated below, these techniques have demonstrated some usefulness.

The anodic polarization studies have shown that pure tungsten and the four alloys studied undergo a transition from an active state to a LC region in all the four solutions used. In aerated distilled water all the alloys behave in a like manner to tungsten. The shapes of the polarization curves in sodium chloride solution clearly show that it has a marked effect on the course of the reaction, and this effect is enhanced by the presence of copper in the alloys. Based on the above trends, the general nature of the corrosion products in distilled water and sodium chloride solution could be predicted. In addition, based on the nature of these curves, the tendency to suffer corrosion through a crevice effect could be predicted.

The instantaneous corrosion rate measurements yielded results for these rates of about the correct order of magnitude.

In the galvanic corrosion studies, for the tungsten/binder-phase system the binder is the anodic material, and this trend persists if there is a two-thirds reduction in the surface area of the binder. Similarly, in the system tungsten/AUS alloy, the alloy is the anodic material. Based on the above trends, the type of corrosion products formed from the alloy AUS in sodium chloride solution can be predicted.

The surface potential mapping studies clearly support a corrosion mechanism [3, 4] based on a bimetallic effect resulting from the presence of the two phases

discrete tungsten particles
binder phase

in these high-density sintered tungsten systems.

Hence some success in the prediction of the corrosion behaviour of these high density sintered tungsten alloys, and pure tungsten, has been achieved by the electrochemical approach. A number of anomalies were observed and it is concluded that this is due to the complex nature of the corrosion processes occurring when these alloys are immersed in distilled water or sodium chloride solution.

6. REFERENCES

1. Batten, J.J. (1988). Delusions of adequacy: the protection of military equipment against degradation. In, Proceedings of the Commonwealth Defence Science Organisation Conference, Kuala Lumpur, Malaysia, February, 1988, General Symposium, Session I (Durability and Life Extension), pp. 1-31.

2. Batten, J.J., McDonald, I.G., Moore, B.T. and Silva, V.M. (1988). Corrosion of high-density sintered tungsten alloys. Part 1. Immersion testing (U). Report MRL-R-1139, Materials Research Laboratory, Melbourne, Victoria.

3. Batten, J.J. and Moore, B.T. (1988). Corrosion of high-density sintered tungsten alloys. In, Proceedings of the Australasian Corrosion Association Conference 28, Perth, Western Australia, November, 1988.

4. Batten, J.J. and Moore, B.T. (1988). Corrosion of high-density sintered tungsten alloys. Part 2. Accelerated corrosion testing (U). Report MRL-R-1145, Materials Research Laboratory, Melbourne, Victoria.

5. Koger, J.W. (1974). Corrosion of tungsten-3.5 nickel-1.5 iron and its constituent phases in aqueous chloride solutions. Preprint γ-DA-6063, Union Carbide Oak Ridge Y-12 Plant, Oak Ridge, Tennessee.

6. Levy, M. and Chang, F. (1981). Corrosion behaviour of high density tungsten alloys. In, Proceedings of the Second International Conference on Environmental Degradation of Engineering Materials in Agressive Environments, September 21-23, 1981, pp. 33-42.

7. Chang, F.C., Levy, M. and Lin, S.S. (1986). The effect of ion implantation on the corrosion behaviour of a high density sintered tungsten alloy. In, Corrosion 86 NACE, Houston, TX.

8. Aylott, P.J., Scantlebury, J.D., Sussex, G.A.M. and Johnson, J.B. (1984). The galvanic corrosion of tungsten and nickel alloys. In, Proceedings of the Ninth International Congress on Metallic Corrosion, Toronto, June 3-7, 1984, Volume 3, pp. 109-114.

9. Standard definitions of terms relating to corrosion and corrosion testing. In, 1986 Annual Book of ASTM Standards, Section 3, Volume 03.02, G15-85a, pp. 135-139.

10. Bombaci, S.A. and Taylor, R.J. (1986). A procedure for the mounting of FeCrNiMo alloy electrodes for electrochemical measurements. Corrosion, 42 (2), 118-119.

11. (a) Standard practice for conventions applicable to electrochemical measurements in corrosion testing.

    (b) Standard practice for standard reference method for making potentiostatic and potentiodynamic anodic polarization measurements.

    In, 1986 Annual Book of ASTM Standards, Section 3, Volume 03.02, G3-74 (Reapproved 1981) and G5-82, pp. 102-110, 124-134.

12. Williams, Lindsay, F.G. (1979). Automated corrosion rate monitoring of zinc in a near-neutral solution using a microcomputer. Corrosion Science, 19, 767-775.

13. Standard guide for conducting and evaluating galvanic corrosion tests in electrolytes. In, 1986 Annual Book of ASTM Standards, Section 3, Volume 03.02, G71-81 (Reapproved 1986), pp. 392-397.

14. O'Halloran, Roger, J., Williams, Lindsay, F.G. and Lloyd, C. Paul (1984). A microprocessor based isopotential contouring system for monitoring surface corrosion. Corrosion, 40, 344-349.

15. Batten, J.J. (1961). Positional effects in the rate of reaction between silver and nitric acid. Aust. J. App. Sci., 12, 358-60.

TABLE 1

Electrochemical Data Derived from Anodic Polarisation Studies on Sintered Tungsten Alloys in Distilled Water or 3.5% Sodium Chloride Solution at Ambient Temperatures

Alloy	Corrosion Potential (mV) (SCE)		Corrosion Current Density ($\mu A\ cm^{-2}$)		Limiting Current Region			
					Potential (mV) (SCE)		Maximum Current Density ($\mu A\ cm^{-2}$)	
	H_2O	NaCl	H_2O	NaCl	H_2O	NaCl	H_2O	NaCl
AERATED SOLUTIONS								
W	-180	-355	<1	<1	20	160	4×10^1	8×10^1
AUS	-250	-320	<1	2	10	180	8×10^1	4×10^2
UK(Fe)	-210	-340	<1	2	0	(a)*	3×10^1	(a)*
UK(Cu)	-180	-330	<1	<1	(a)*	70	(a)*	5×10^3
US	-210	-340	<1	3	20	100	8×10^1	8×10^3
Binder	-260	-310	<1	<0.2	(a)*	-170	(a)*	3×10^3
DE-AERATED SOLUTIONS								
W	-500	-550	1	1.5	20	120	4×10^1	7.5×10^1
AUS	-510	-540	1	3	90	150	5×10^1	2×10^2
UK(Fe)	-580	-630	1	5	250	-140	5×10^1	3×10^3
UK(Cu)	-480	-475	5	3	150	70	2×10^3	4×10^3
US	-400	-560	<1	3	20	70	5×10^1	1×10^4
Binder	-420	-610	<1	1	(a)*	-150	(a)*	1.8×10^3

(a)* No limiting current region.

TABLE 2

Average Instantaneous Corrosion Rates of Tungsten, the Four Tungsten Alloys and the Binder Phase in AUS in 3.5% Sodium Chloride Solution. Measurements made over a period of five days.

Alloy	Instantaneous Corrosion Rate (mil/yr)	Previous Results from Immersion Tests [1-4] (mil/yr)
W	0.10	0.02
AUS	0.51	0.2
UK(Fe)	0.35	0.2
UK(Cu)	0.06	0.3
US	0.29	0.5
Binder	0.13	-

TABLE 3

Influence of Time of Immersion on the Corrosion Potentials of Pure Tungsten, the Tungsten Alloy AUS and its Binder Phase in Sodium Chloride Solution and in Distilled Water at Ambient Temperatures

Time of Immersion (days)	Corrosion Potential (mV) (SCE)		
	Pure tungsten	Australian binder phase	Australian alloy
IN 5% SODIUM CHLORIDE SOLUTION			
1	-260	-350	-300
7	-260	-400	-330
30	-260	-420	-340
60	-245	-445	-345
90	-235	-455	-340
120		-450	
150		-455	
IN DISTILLED WATER			
1	-295	-335	-350
2	-300	-390	-355
3 (am)	-300	-395	-355
(pm)	-305	-390	-360
12	-310	-320	-355
		-320	
		-305	
		-300	
16	-305	-320	-360
30	-305	-325	-355
44	-260	-330	-350
45	-260	-330	-350
72	-235	-315	-330
74	-195	-290	-375

TABLE 4

Galvanic Corrosion Studies Involving Pure Tungsten, the Tungsten Alloy AUS and its Binder Phase in 5% Sodium Chloride Solution at Ambient Temperatures

Electrochemical Cell in Sodium Chloride Solution and Relative Surface Areas	Corrosion Potentials of the Uncoupled Electrodes (mV) (SCE)		Electrochemical Cell*			
			Mixed potential (mV) (SCE)		Galvanic current (μA)	
			Initial	Stable**	Initial	Stable**
Tungsten/Binder phase	Tungsten	Binder phase				
4:1	-260	-420	-370 (-360)	-370 (-360)	30 (11.4)	7.7 (10.8)
4:0.3	-280	-365	-340	-365 (-345)	1.6	2.2 (2.5)
Tungsten/AUS alloy	Tungsten	AUS alloy				
1:1	-270	-355	-320 (-325)	-330 (-320)	25 (1.7)	1.4 (2.3)
AUS alloy/Binder phase	AUS alloy	Binder phase				
1:1	-340	-390	-385 (-370)	-390 (-360)	15 (1.8)	2 (0.1) (not steady)

* Numbers in brackets are for agitated solutions

** After one to two hours immersion

TABLE 5

Galvanic Corrosion Studies Involving Pure Tungsten, the Tungsten Alloy AUS and its Binder Phase in Distilled Water at Ambient Temperature

Electrochemical Cell in Distilled Water and Relative Surface Areas	Corrosion Potentials of the Uncoupled Electrodes (mV) (SCE)		Electrochemical Cell*			
			Mixed potential (mV) (SCE)		Galvanic current (μA)	
			Initial	Stable**	Initial	Stable**
Tungsten/Binder phase	Tungsten	Binder phase				
4:1	-230	-370	-260 (-250)	-265 (-150)	2 (0.5)	0.5 (0.6)
4:0.3	-170	-320	-235 (-270)	-285 (-270)	2.6 (13.3)	11.2 (13.0)
Tungsten/AUS alloy	Tungsten	AUS alloy				
1:1	-220	-350	-290 (-285)	-305 (-265)	2.5 (0.9)	0.9 (0.94)
AUS alloy/Binder phase	AUS alloy	Binder phase				
1:1	-350	-370	-355 (-330)	-355 (-310)	0.3 (0.09)	0.04 (0.1)

* Numbers in brackets are for agitated solutions

** After one to two hours immersion

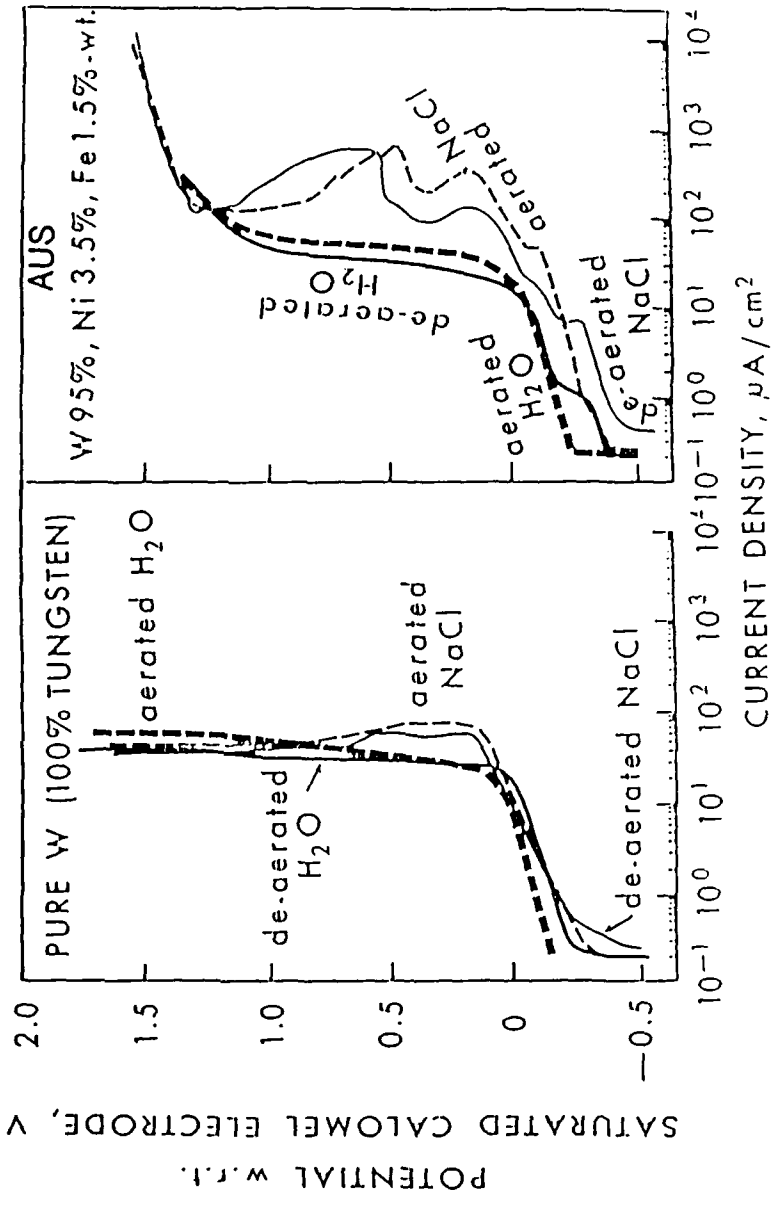

FIGURES 1 and 2 Anodic polarization curves of pure tungsten (Fig. 1) and the sintered tungsten alloy AUS (Fig. 2) in various electrolytes.

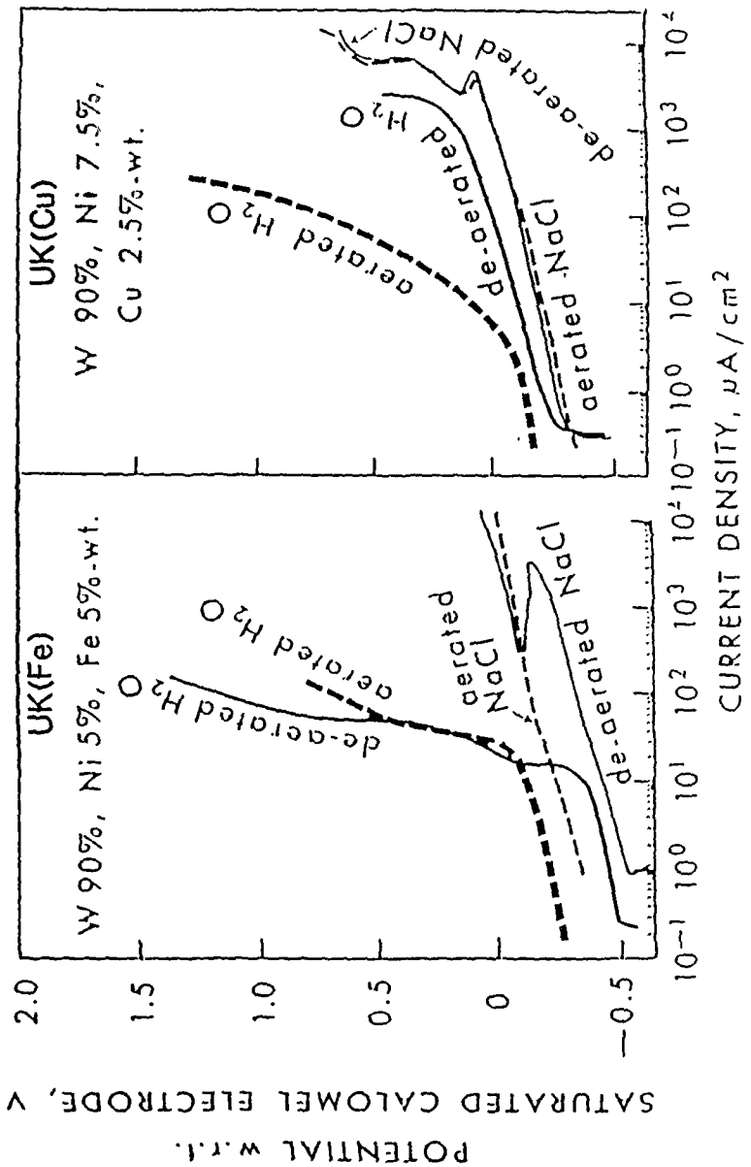

FIGURES 3 and 4 Anodic polarization curves of the sintered tungsten alloys UK(Fe) (Fig. 3) and UK(Cu) (Fig. 4) in various electrolytes.

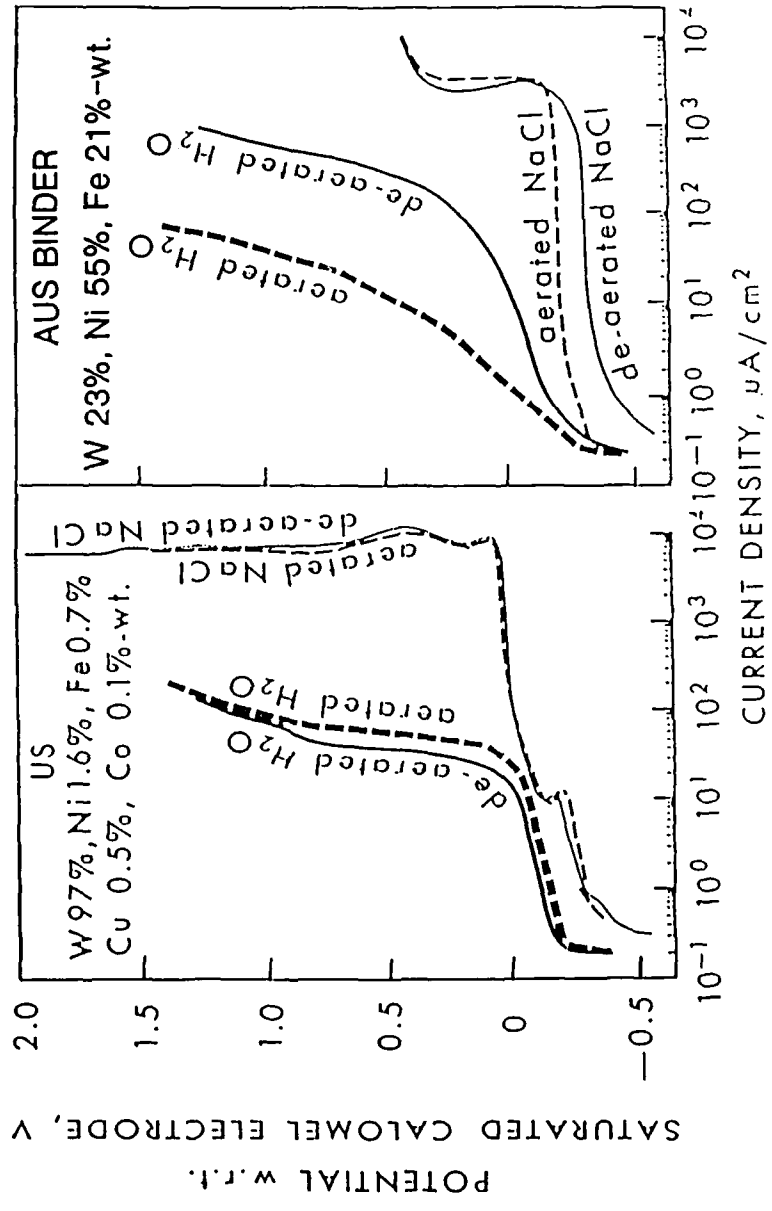

FIGURES 5 and 6 **Anodic polarization curves of the sintered tungsten alloy US (Fig. 5) and the AUS binder (Fig. 6) in various electrolytes.**

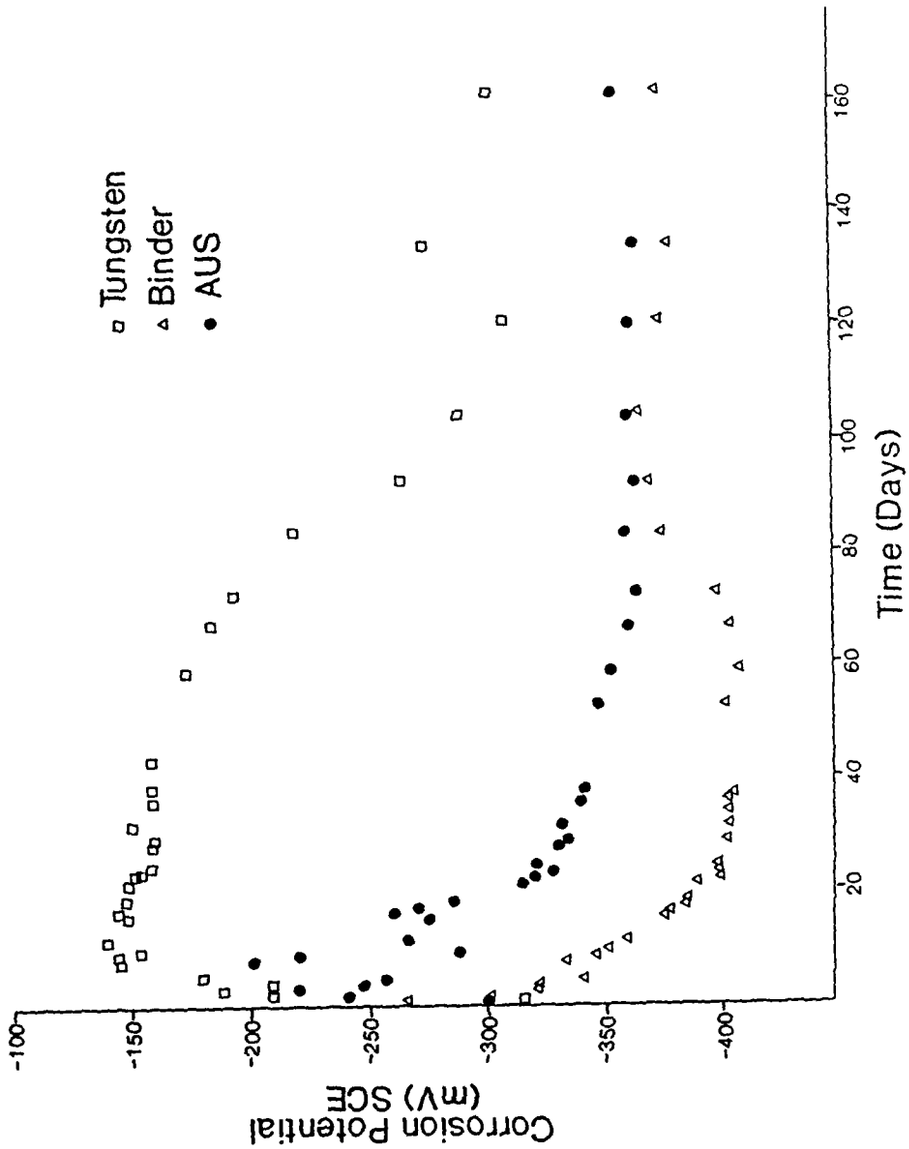

FIGURE 7 Corrosion potential plotted against time of immersion in distilled water for pure tungsten, the Australian alloy (AUS) and its binder phase.

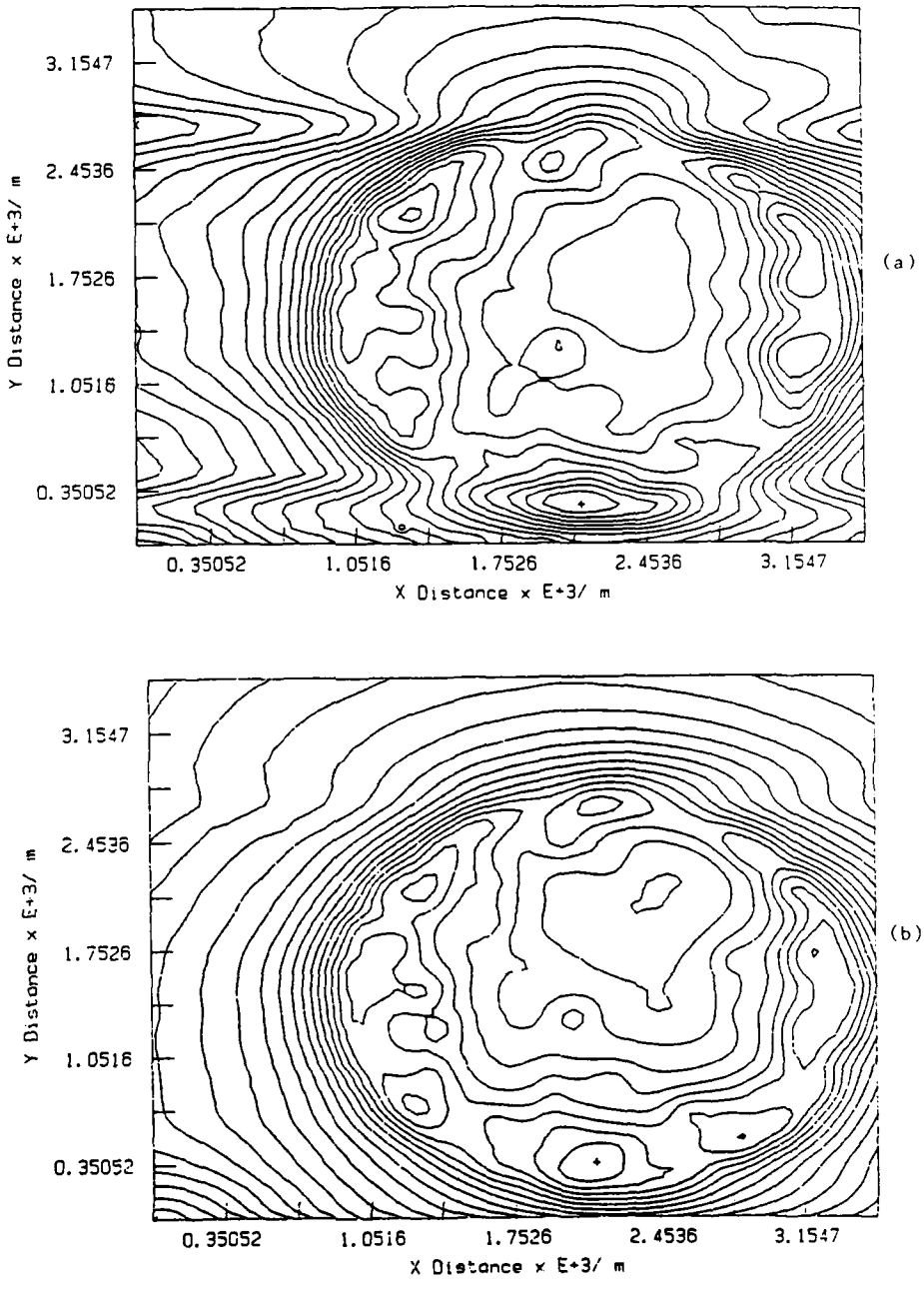

FIGURE 8 Potential scans above a tungsten surface containing a circular insert of AUS binder (cf. Figure 9). Time of immersion (a) 1 hour, (b) 4 hour, in 2.5×10^{-4} M sodium chloride solution.

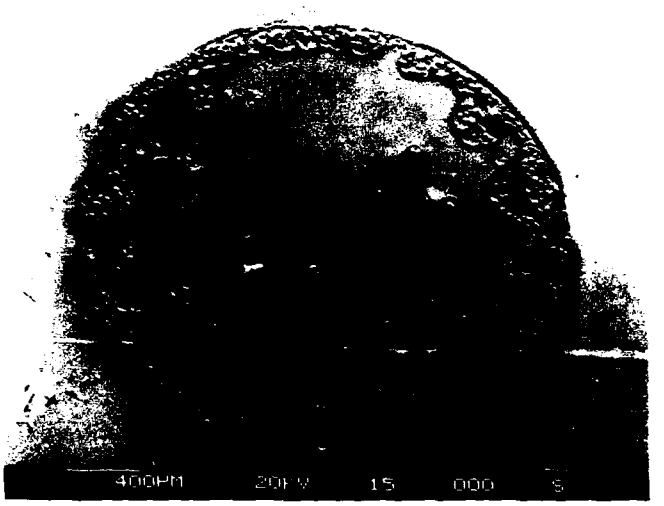

FIGURE 9 Photomicrograph of the surface showing the area scanned by the reference electrode (cf. Figure 8). The circular region is the AUS binder and this is imbedded in pure tungsten. Time of immersion, 4 hours in 2.5×10^{-4} M sodium chloride solution.

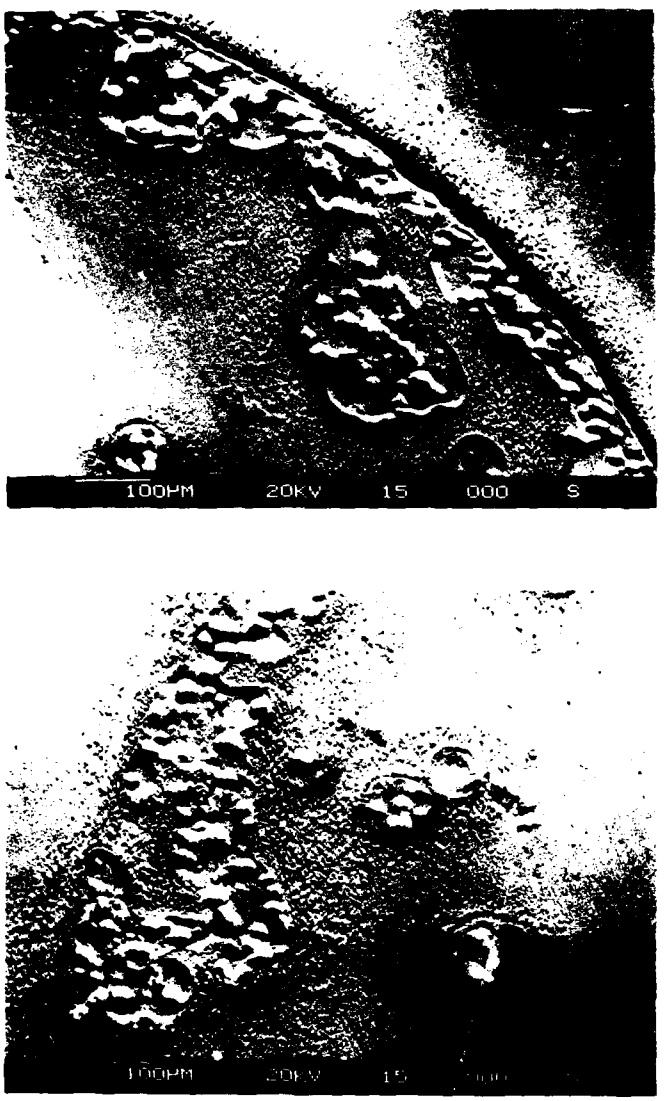

(a)

(b)

FIGURE 10 Photomicrograph of part of the surface of the area scanned (Figure 9) showing (a) corrosion products on the binder insert and a crevice between the insert and the tungsten surface, and (b) another area of the binder insert showing corrosion products at the periphery but there does not appear to be a crevice between the binder and the surrounding tungsten.

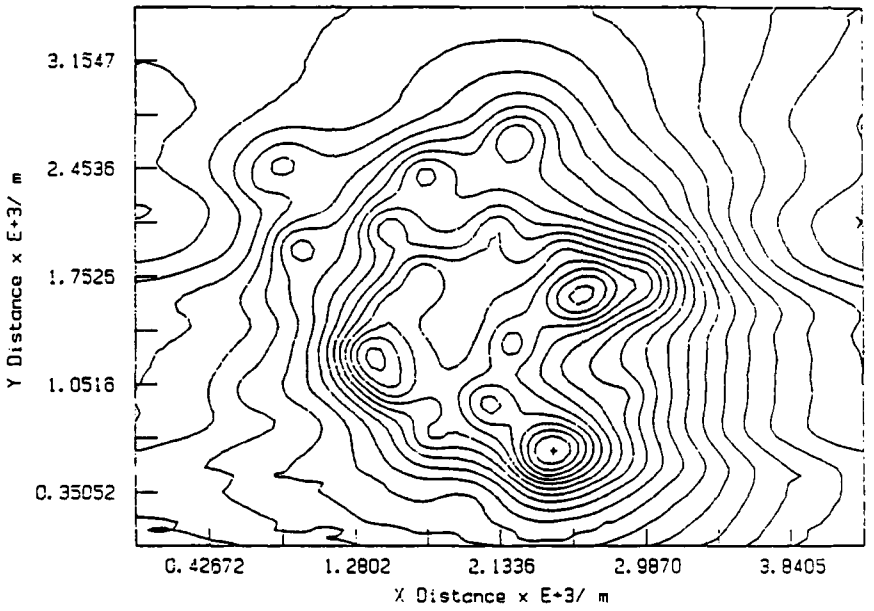

FIGURE 11 Typical of the potential scans obtained when the reference electrode moved above the surfaces of tungsten and AUS binder separated by mounting resin (see Figure 12) but connected on their back faces by a conducting polymer. Time of immersion, up to 4 hours in 2.5 x 10^{-4} M sodium chloride solution. In this figure, the gap between the binder and the tungsten corresponds (approximately) with the x co-ordinates 3.4 and 3.8.

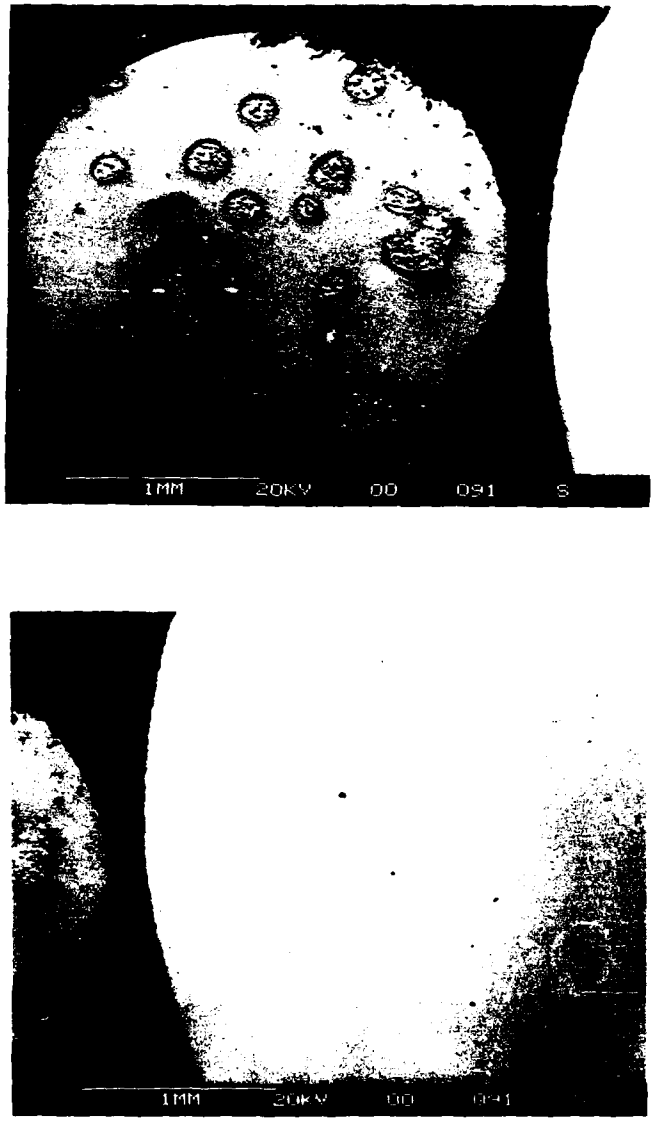

FIGURE 12 Photomicrographs of the surfaces of AUS binder and pure tungsten (LHS & RHS respectively of the micrographs) mounted together in bakelite and connected electrically on their back faces. Time of immersion, 4 hours in 2.5×10^{-4} M sodium chloride solution.

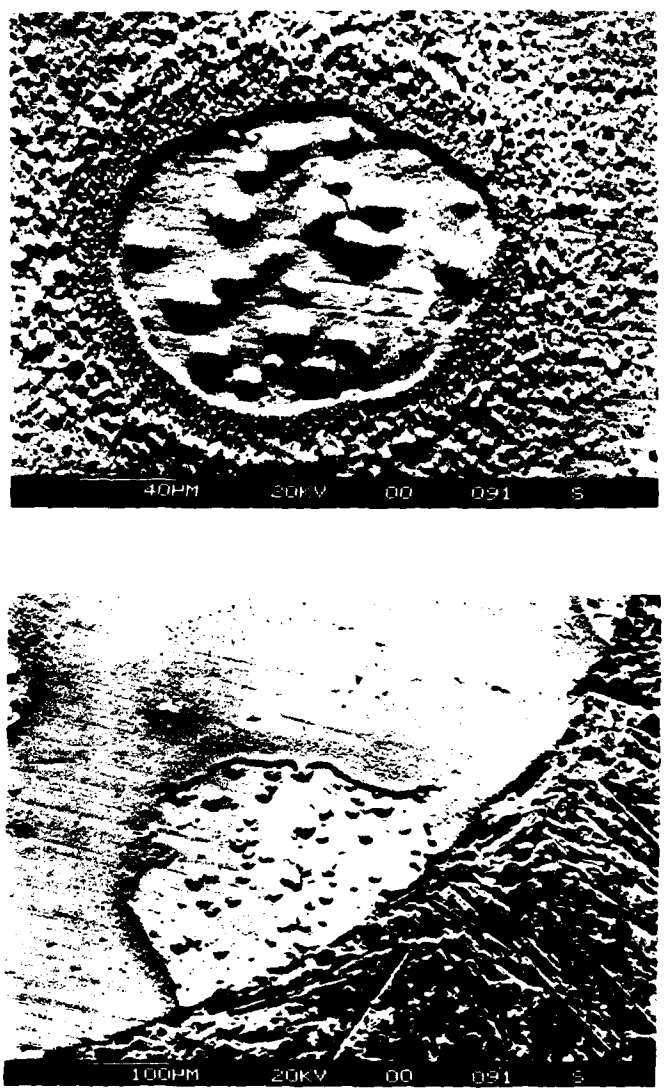

(b)

FIGURE 13 Two of the corrosion spots on the AUS binder shown in Figure 12. Note the creviced area between the binder and the mounting resin in (b).

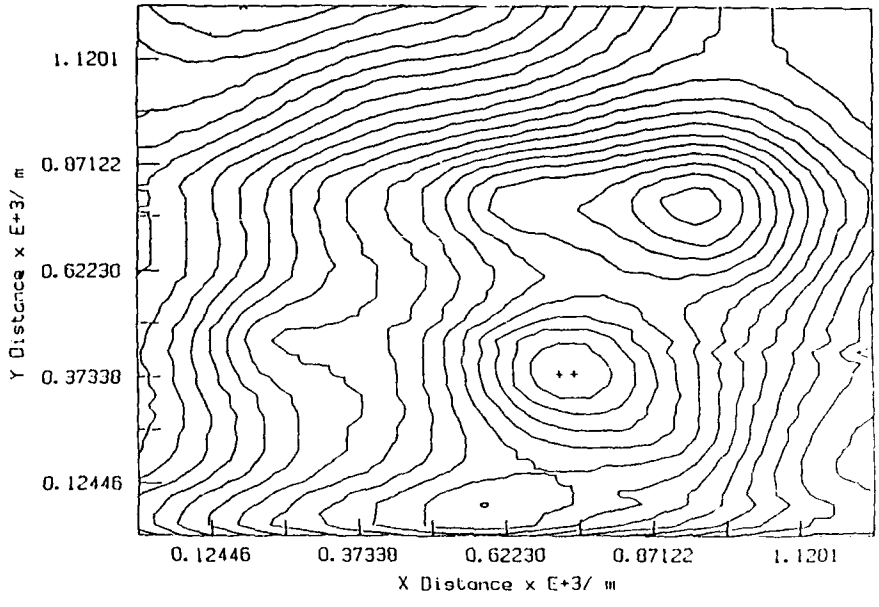

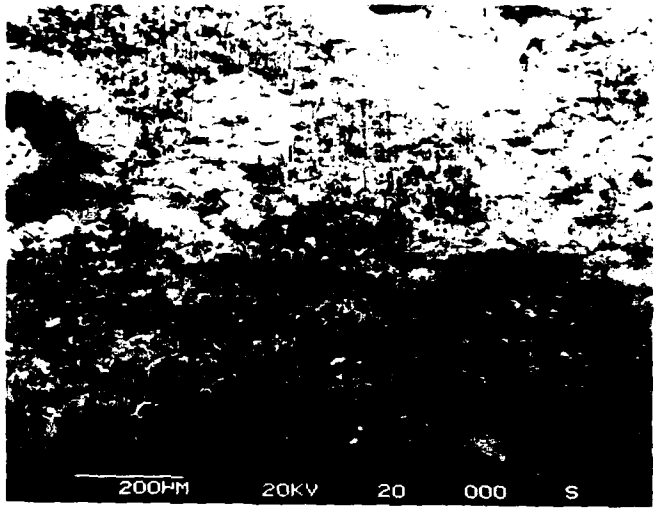

FIGURE 14 (upper) Typical of the isopotential contour maps obtained for the tungsten alloy AUS over a period of about 4 weeks immersion in 2.5×10^{-4} M sodium chloride solution.

FIGURE 15 (lower) Photomicrograph of the surface of the tungsten alloy AUS after seventy days immersion in distilled water and after removal of corrosion products. A similar pattern of attack (i.e. non-uniform) was obtained after immersion in 5% sodium chloride solution.

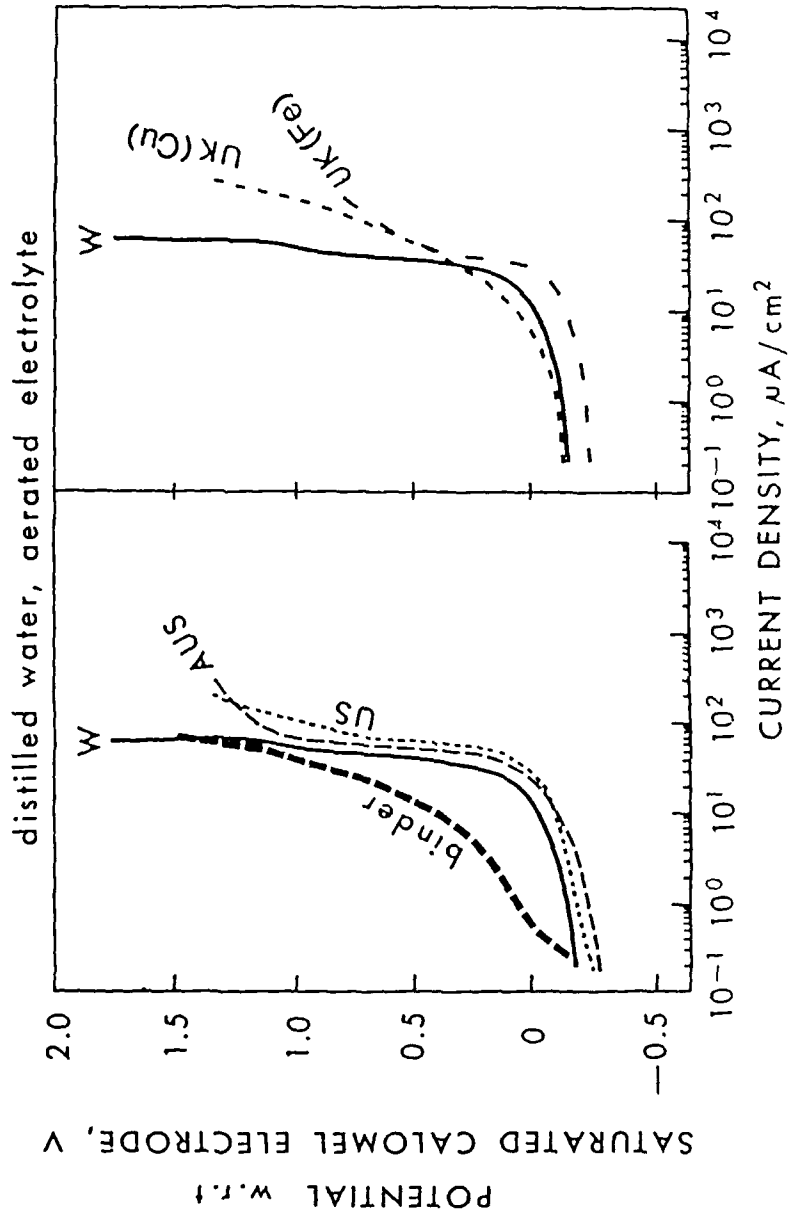

FIGURE 16 Anodic polarization curves of tungsten, the sintered tungsten alloys and the AUS binder in aerated distilled water.

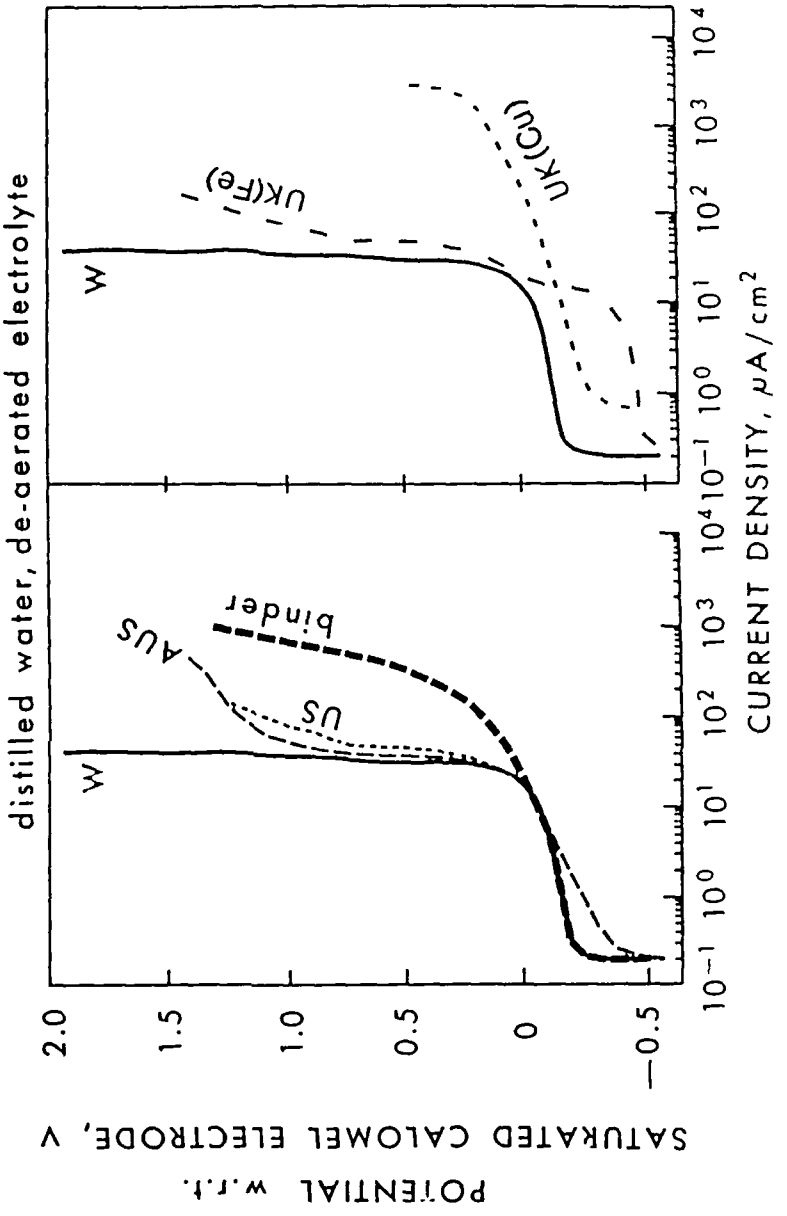

FIGURE 17 Anodic polarization curves of tungsten, the sintered tungsten alloys and the AUS binder in de-aerated distilled water.

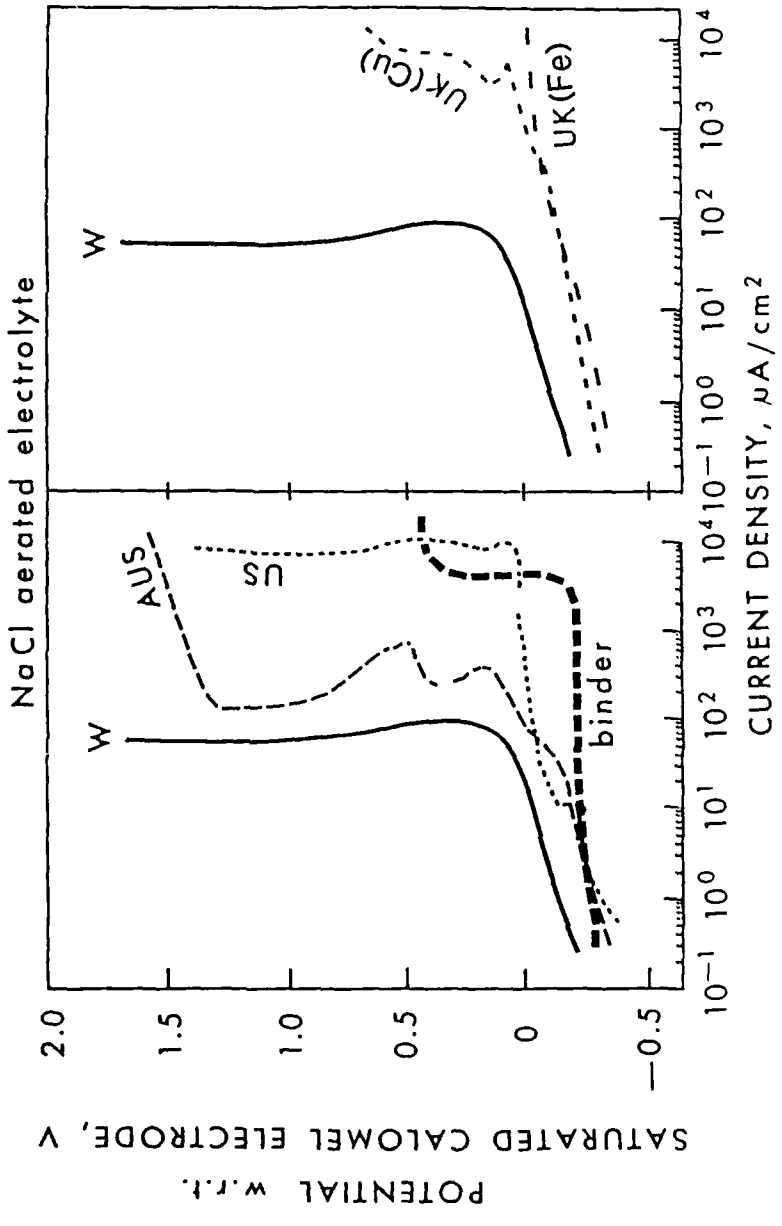

FIGURE 18 Anodic polarization curves of tungsten, the sintered tungsten alloys and the AUS binder in aerated sodium chloride solution.

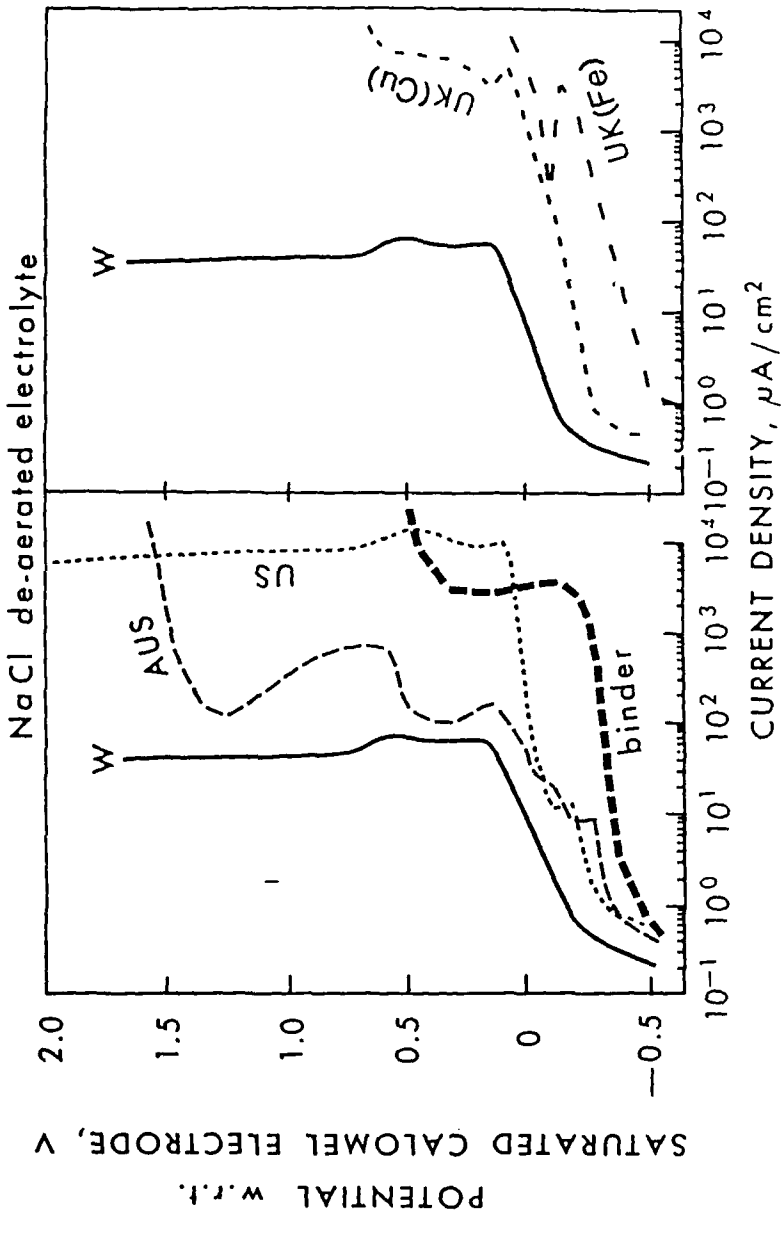

FIGURE 19 Anodic polarization curves of tungsten, the sintered tungsten alloys and the AUS binder in de-aerated sodium chloride solution.

SECURITY CLASSIFICATION OF THIS PAGE **UNCLASSIFIED**

DOCUMENT CONTROL DATA SHEET

REPORT NO.	AR NO.	REPORT SECURITY CLASSIFICATION
MRL-R-1146	AR-005-671	Unclassified

TITLE

Corrosion of high-density sintered tungsten alloys
Part 3: Electrochemical tests

AUTHOR(S)

J.J. Batten, S.A. Bombaci, W.N.C. Garrard, B.T. Moore and B.S. Smith

CORPORATE AUTHOR

Materials Research Laboratory
Defence Science & Technology Organisation
PO Box 50
Ascot Vale Victoria 3032

REPORT DATE	TASK NO.	SPONSOR
December 1988	NAV 86/086	RAN

FILE NO.	REFERENCES	PAGES
G6/4/8-3557	15	43

CLASSIFICATION/LIMITATION REVIEW DATE

CLASSIFICATION/RELEASE AUTHORITY
Chief, Protective Chemistry Division MRL

SECONDARY DISTRIBUTION

Approved for Public Release

ANNOUNCEMENT

Announcement of this report is unlimited

KEYWORDS

Corrosion Tungsten alloys

SUBJECT GROUPS 0071G

ABSTRACT

The corrosion behaviour of tungsten and high-density tungsten alloys (W $\geq$ 90 weight %) has been examined electrochemically through anodic polarization measurements, instantaneous corrosion rate measurements, galvanic coupling, and surface potential mapping. In the anodic polarization tests, pure tungsten and the four alloys studied underwent transitions from an active state to a state where any further increase in potential produced no further increase in current. The presence of chloride ions increased corrosion rates.

Predictions of likely trends in corrosion rates from the above electrochemical tests were not in complete agreement with those obtained by the long-term immersion tests. Similarly, a consistent prediction of the likely nature of the corrosion products that would result from long-term immersion testing was not obtained from the above studies. Predictions about which alloys would be susceptible to a crevice effect were in agreement with the immersion testing results, namely those alloys not containing Cu would be the most susceptible.

Some insight into the nature of the corrosion mechanism is afforded by the work on galvanic coupling and surface potential mapping: this supported the view that galvanic corrosion plays a part in the corrosion process.